Author/s:
O'Hair, RAJ;Mravak, A;Krstić, M;Bonačić-Koutecký, V

Title:
Models Facilitating the Design of a New Metal-Organic Framework Catalyst for the Selective Decomposition of Formic Acid into Hydrogen and Carbon Dioxide

Date:
2019-05-20

Citation:
O'Hair, R. A. J., Mravak, A., Krstić, M. & Bonačić-Koutecký, V. (2019). Models Facilitating the Design of a New Metal-Organic Framework Catalyst for the Selective Decomposition of Formic Acid into Hydrogen and Carbon Dioxide. Chemcatchem, 11 (10), pp.2443-2448. https://doi.org/10.1002/cctc.201900346.

Persistent Link:
https://hdl.handle.net/11343/285819

Author Manuscript

Title: Models facilitating the design of a new metal-organic framework catalyst for the selective decomposition of formic acid into hydrogen and carbon dioxide.

Authors: Richard A J O'Hair, PhD DSc; Antonija Mravak; Marjan Krstić; Vlasta Bonacic-Koutecky

To be cited as: 10.1002/cctc.201900346

Link to VoR: https://doi.org/10.1002/cctc.201900346

Models facilitating the design of a new metal-organic framework catalyst for the selective decomposition of formic acid into hydrogen and carbon dioxide.

Richard A. J. O'Hair,*[a] Antonija Mravak, [b] Marjan Krstić [b] and Vlasta Bonačić-Koutecký*[b,c]

Dedicated to Professor Veronica Bierbaum on the occasion of her retirement.

Abstract: Here we describe a new conceptual approach for the design of a heterogeneous metal-organic framework (MOF) catalyst based on UiO-67 for the decomposition of formic acid in context of hydrogen storage, a reaction with important application in hydrogen storage and *in situ* generation of H_2. Models for the {CuH} reactive catalytic site at the organic linker are assessed. In the first model system, gas-phase mass spectrometry experiments and DFT calculations on a fixed charge bathophen ligated copper hydride complex, $[(phen^*)Cu(H)]^{2-}$, were used to demonstrate that it acts as a catalyst for the selective decomposition of formic acid into H_2 and CO_2 via a two step catalytic cycle. In the first step liberation of H_2 to form the carboxylate complex, $[(phen^*)Cu(O_2CH)]^{2-}$ occurs, which in the second step selectively decomposes via CO_2 extrusion to regenerate the hydride complex. DFT calculations on four other model systems showed that changing the catalyst to neutral [(LCu(H)] complexes or embedding it within a MOF results in mechanisms which are essentially identical. Thus catalytic active sites located on the organic linker of a MOF appear to be close to a gas-phase environment, thereby benefitting from the favorable characteristics of gas-phase reactions and validating the use of gas-phase models to design new MOF based catalysts.

Introduction

Thirty years ago Robson proposed the rational design and construction of a novel class of porous materials composed of metal centres as nodes that connect to organic ligands as rods (linkers) [1,2]. In two landmark papers he provided remarkable visions for a new field of chemistry for these coordination polymers [3], which were subsequently rebranded as metal-organic frameworks (MOFs) [4]. He noted that "*despite Nature's abhorrence of a vacuum it may be possible to devise rods with sufficient rigidity to support the existence of solids with relatively huge empty cavities*" and prophesised that "*relatively unimpeded migration of species throughout the lattice {MOF} may allow chemical functionalization of the rods {linkers} subsequent to the construction of the framework. The introduction of one or more catalytic centers per rod may thereby be straightforward. The very open structure should again ensure both easy access of substrates to catalytic sites and ready release of catalytic products*". The prediction of post-synthetic modification (PSM) of a MOF [5] to build a supported catalyst had to wait over a decade until Lin's pioneering work on a MOF based heterogeneous asymmetric catalyst for the addition of diethyzinc to aromatic aldehydes to afford chiral secondary alcohols [6].

[a] Prof. Richard A. J. O'Hair
School of Chemistry and BIO21 Molecular Science and Biotechnology Institute
30 Flemington Rd, Parkville, Victoria 3010 (Australia),
E-mail: rohair@unimelb.edu.au

[b] A. Mravak, Dr. M. Krstić, Prof. V. Bonačić-Koutecký
Center of Excellence for Science and Technology – Integration of Mediterranean Region (STIM) at Interdisciplinary Center for Advanced Sciences and Technology (ICAST), University of Split
Poljička cesta 35, 21000 Split (Croatia)

[c] Prof. V. Bonačić-Koutecký
Chemistry Department,
Humboldt University of Berlin
Brook – Taylor – Strasse 2, 12489 Berlin (Germany)
E-mail: vbk@cms.hu-berlin.de

Supporting information for this article is given via a link at the end of the document.

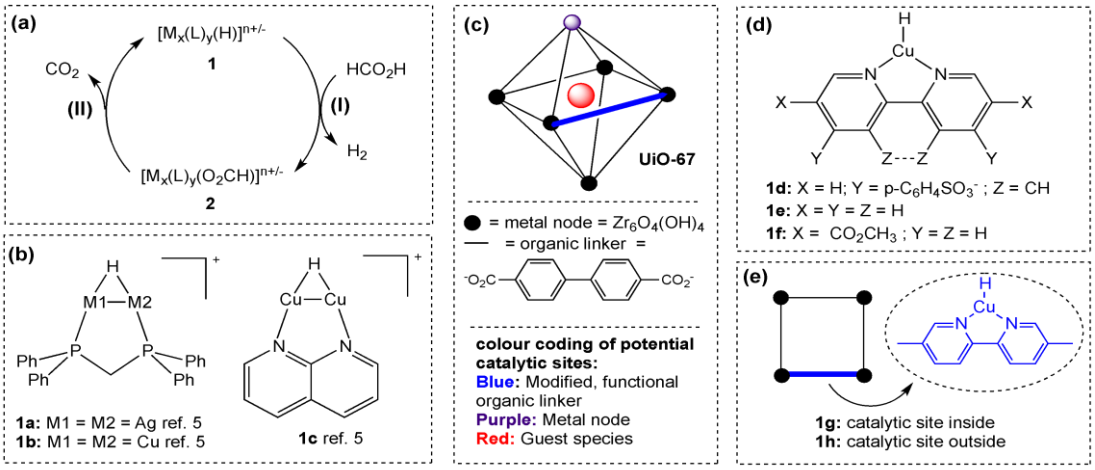

Scheme 1. Design principles for coinage metal hydrides for the selective decarboxylation of formic acid: (a) two-step catalytic cycle. Step (I) is an ion-molecule reaction with formic acid; Step (II) involves liberation of CO_2 under CID conditions. (b) 1st (**1a**), 2nd (**1b**) and 3rd (**1c**) generation gas-phase binuclear coinage metal hydride catalysts previously reported. (c) examples of potential catalytic sites within the MOF **UiO-67**; (d) Gas-phase models for mononuclear copper hydride catalysts located at the organic linker; (e) models for the heterogenization of a gas-phase homogenous catalyst located at the organic linker in a MOF.

Although much progress has since been made in constructing a wide range of MOF catalysts [7], the vacuum like environment within MOFs suggested to us a tantalizing new concept for the design of novel MOF based catalysts, where gas-phase studies are used to examine the likely reactivity of a catalytic metal site within a MOF (Scheme 1). The use of gas-phase models seemed plausible given that our previous reaction-mechanisms approach, where gas-phase studies using multistage mass spectrometry experiments (MS^n) in an ion trap are blended with DFT calculations [8], was successfully applied to the design of new catalysts from the ground up [9-12] and the invention of new reactions for use in organic synthesis [13]. In the former studies, through a sequence of iterations in which different ligands and metal sites were evaluated, we developed a series of ligated binuclear coinage metal hydride cationic catalysts for the selective decarboxylation of formic acid (Scheme 1a, b) [14], a reaction of considerable interest for the use of formic acid in hydrogen storage applications [15]. In all cases a two-step catalytic cycle operates (Scheme 1a) in which the metal hydride complex, **1**, reacts in **Step I** with formic acid to liberate hydrogen and form a coordinated metal formate, **2**, which in **Step II** liberates CO_2 under conditions of collision-induced dissociation (CID). For these first generation catalysts the best ligand for the silver hydride was 1,1-bis(diphenylphosphino)methane (dppm) to give complex **1a** (Scheme 1b), and solution phase studies confirmed the liberation of H_2 and CO_2 at a relatively low temperature of 65 ^oC [9]. Although the exact nature of the stoichiometry of the solution phase catalysts is unknown, subsequent gas phase studies highlighted that tetranuclear silver hydride cluster complexes were unreactive towards formic acid [10]. This spurred us onto examining the role of the metal centre, where all possible homo and hetero coinage metal complexes were explored to establish that the best gas-phase catalyst for both steps in the catalytic cycle was the biscopper complex **1b** [11]. Given the difficulty of establishing the nature of the solution phase catalyst, we were interested in translating the gas-phase homogeneous catalysts into a heterogenous system. Unfortunately, the second generation catalyst **1b** was shown by DFT calculations not to fit into the framework of a ZSM-5 zeolite, which resulted in the development of a new, less bulky catalyst **1c** based upon the N-based 1,8-naphthyridine ligand [12]. This catalytic site was found to fit neatly into the framework a ZSM-5 zeolite. Due to the experimental challenges of developing these zeolite based “ship in a bottle” catalysts [16], we were tempted by the “heterogenization of a homogenous catalyst” strategy to use gas-phase studies to design a MOF based catalyst where the metal site is part of the framework. There are three types of potential catalytic sites within a MOF as illustrated for the UiO-67 MOF (Scheme 1c): (i) the organic linker, which can be functionalized to introduce a catalytic site as per Robson’s original proposal; (ii) the metal node; (iii) insertion of a guest catalyst (essentially a “ship in a bottle” catalyst). While all three types of MOF catalysts have been developed [7], we were attracted to developing organic linkers functionalized by a copper hydride catalytic site. Here we use DFT calculations to show that the mechanisms and energetics associated with the two-step catalytic cycle of simple gas-phase catalysts **1d** – **1f** (Scheme 1d) are very similar to those of the models **1g** and **1h** of UiO-67 MOF (Scheme 1e).

Results and Discussion

Since there are no known 1,8-naphthyridine based ligands for the construction of MOFs that would support a binuclear $\{Cu_2H\}^+$ catalytic site related to **1c**, we decided to adopt the 5,5'-dicarboxy-2,2'-bipyridine ligand as an organic linker since: (i) it has been shown to be able to be incorporated into the robust UiO-67 MOF [17]; (ii) PSM of such MOFs with metal sites have been used to prepare catalysts [18]. We first wanted to use experiment and theory in concert to establish that a mononuclear hydride {CuH} complex could act as a catalyst for

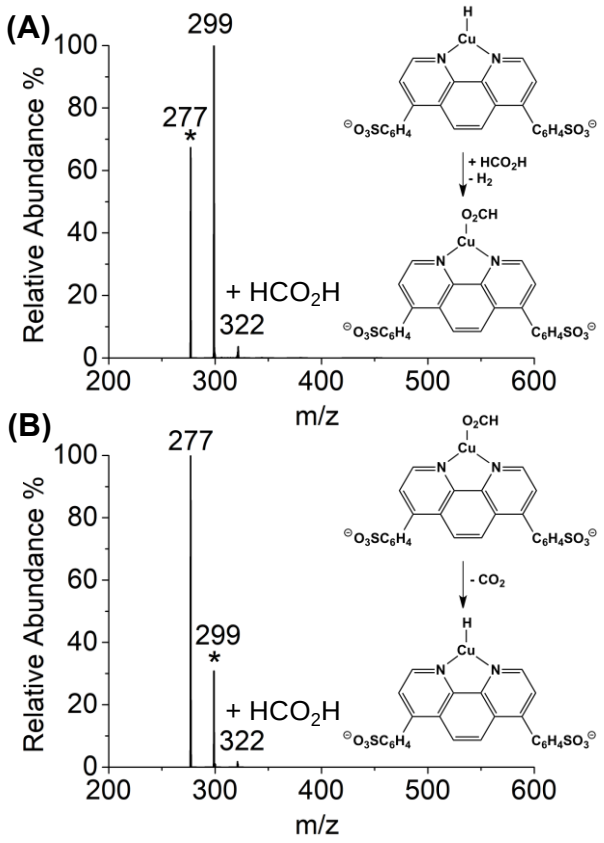

Figure 1. LTQ mass spectra obtained for the MS^n CID (or IMR) experiments of: (a) IMR of $[(phen^*)^{63}Cu(H)]^{2-}$ (m/z 277), **1d**, with formic acid; (b) CID of $[(phen^*)^{63}Cu(O_2CH)]^{2-}$ (m/z 299), **2d**. An activation time of 30 ms was used for the CID experiments and 500 ms for the IMR experiments. A * represents the mass-selected precursor ion.

the selective decarboxylation of formic acid. Since the {CuH} sites in MOFs have no net charge while the mass spectrometry experiments require the use of ions for mass-selection, reaction and detection, we turned to the well-established use of fixed charge ligands.[19] We chose 4,7-diphenyl-1,10-phenanthroline-disulfonic acid disodium salt as the fixed charge ligand (phen*) since it should allow ready formation of the copper formate complex **2d** via electrospray ionization (ESI) and the sulfonate sites: (i) are well away from the {CuH} reactive site and should not significantly perturb reactivity; (ii) have a low gas-phase basicity and should not deprotonate formic acid [20]. Gratifyingly **1d** was readily formed via CID of **2d** and reacts cleanly with formic acid to give the formate complex (eq. 1 and Figure 1a) at the collision rate, consistent with DFT calculations which predict that the reaction is exothermic by 1.07 eV and has a barrier lying below the separated reactants (as discussed further below). No proton transfer is observed (eq. 2), consistent with the low basicity of the chosen sulfonate fixed charges [20] and with DFT calculations which predict that the reaction is endothermic by 0.48 eV. A minor secondary product is formed by reaction of formic acid with the copper formate complex **2d** (eq. 3) as confirmed by mass selection of *m/z* 299 and this adduct fragments via formic acid loss upon CID (data not shown). CID of $[(phen^*)Cu(O_2CH)]^{2-}$ cleanly regenerates $[(phen^*)Cu(H)]^{2-}$ via decarboxylation (eq. 4).

$$[(phen^*)Cu(H)]^{2-} + HCO_2H \rightarrow [(phen^*)Cu(O_2CH)]^{2-} + H_2 \quad (1)$$

$$[(phen^*)Cu(H)]^{2-} + HCO_2H \rightarrow [(phen^* + H)Cu(H)]^{-} + HCO_2^{-} \quad (2)$$

$$[(phen^*)Cu(O_2CH)]^{2-} + HCO_2H \rightarrow [(phen^*)Cu(O_2CH)(HCO_2H)]^{2-} \quad (3)$$

$$[(phen^*)Cu(O_2CH)]^{2-} \rightarrow [(phen^*)Cu(H)]^{2-} + CO_2 \quad (4)$$

Figure 2. DFT-calculated energy profile for the two reaction steps in the catalytic cycle for $[(phen^*)Cu(H)]^{2-}$, **1d** in the gas-phase. All structures were fully optimized using DFT method with the hybrid B3LYP functional and def2-TZVP atomic basis set which has been used for all atoms. Color coding of atoms: green – carbon, red – oxygen, white – hydrogen, blue – nitrogen, yellow – sulfur, brown – copper.

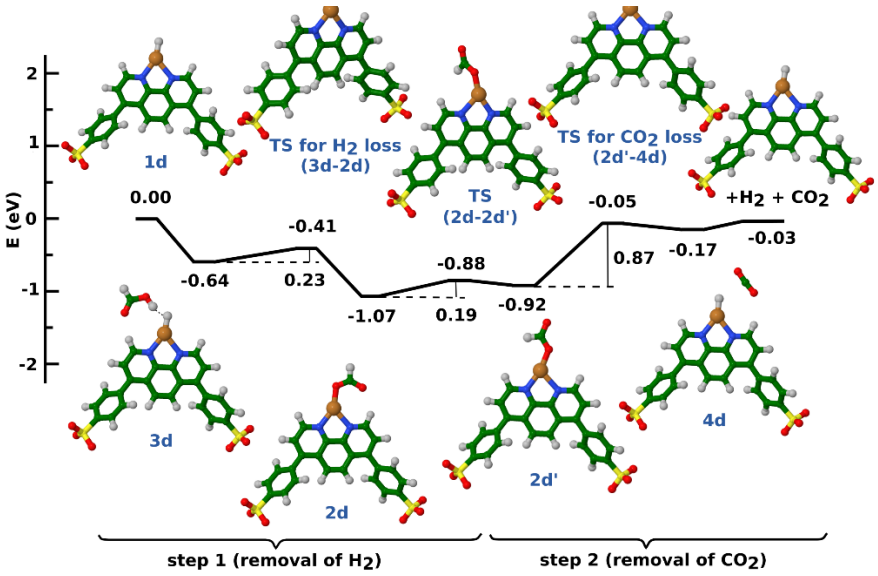

all key species for all model systems. The most noteworthy

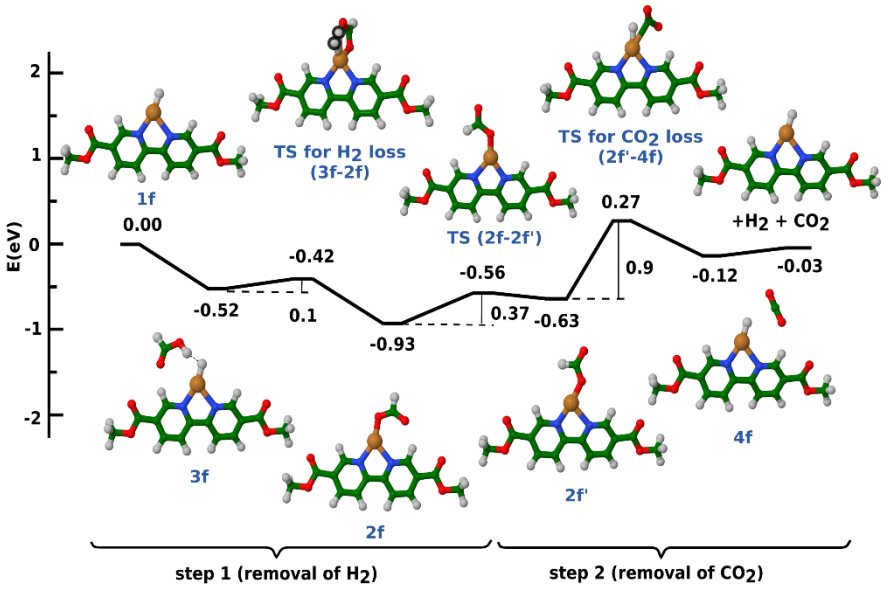

In order to examine the mechanistic aspects responsible for the selective decomposition of formic acid into H_2 and CO_2 via reaction steps **I** and **II** within the catalytic cycle (Scheme 1a), DFT energy profiles have been determined for five systems: (i) $[(phen^*)Cu(H)]^{2-}$, **1d** (Scheme 1d), which has been experimentally investigated in gas phase (Figure 1), (ii) [(bipy)Cu(H)], **1e** (Scheme 1d); (iii) [(bipy*)Cu(H)], **1f** (Scheme 1d), which contains the organic linker present in MOF UiO-67, and capped as a diester; and models for MOF UiO-67 [21] in which the octahedron is simplified as a square consisting of three biphenyl organic linkers, one (bipy*)Cu(H) organic linker containing the catalytic site and four $Zr_6O_4(OH)_4(COOH)_{10}$ nodes in the corners, with the CuH catalytic pointing (iv) into the centre of the square, [UiO-67(bipy)Cu(H)in], **1g** (Scheme 1e); (v) outside of the square, [UiO-67(bipy)Cu(H)out], **1h** (Scheme 1e). The DFT calculated energy profiles are shown in Figures 2, S2, 3, 4 and S4 respectively and Table 1 compares the energies of aspect of comparing the energy profiles and associated structures is that the mechanistic features are similar for all model systems, with small perturbations to the energetics. In all cases the formic acid binds to the CuH catalytic center to generate complex **3**. For step I breaking of the formic acid O-H bond and formation of H_2 occurs over an energy barrier associated with **TS3-2**, which is below the energy at the separated reactants in the case of all the gas phase systems (**1d** , **1e** and **1f**) while for the MOF models **1g** and **1h**, the formation of **2** with concomitant release of H_2 occurs without a barrier (cf. Figures 2-4). In all cases loss of H_2 to form the copper formate subunit, CuO_2CH is energetically favorable. For the first step of the reaction, the N,N-bidentate {CuH} subunit represents the key reactive site consistent with the calculated HOMOs (Figure S3).

For the loss of CO_2 associated with **step II** and to close the catalytic cycle, two energy barriers have to be overcome. **TS2-2'** is associated with the required conformational change of the formate ligand to form the reactive conformer **2'** for decarboxylation, which surmounts **TS2'-4** to yield the hydride complex **4**, in which CO_2 is loosely interacting (with Cu-O distance of around 3.7 Å) and from which CO_2 is readily lost to generate **1**.

Table 1. Summary of key energies associated with Steps I and II for all systems studied.

Figure 3. DFT-calculated energy profile for the two reaction steps in the catalytic cycle for [(bipy*)Cu(H)], **1f** in the gas-phase. All structures were fully optimized using DFT method with the hybrid B3LYP functional and def2-TZVP atomic basis set which has been used for all atoms. Color coding of atoms: green – carbon, red – oxygen, white – hydrogen, blue – nitrogen, brown – copper.

[(bipy)Cu(H)], **1e** [c]	-0.61	-0.41 (0.2)	-1.01	-0.61 (0.4)	-0.67	0.18 (0.85)	-0.15
[(bipy*)Cu(H)], **1f** [c]	-0.52	-0.42 (0.1)	-0.93	-0.56 (0.37)	-0.63	+0.27 (0.9)	-0.12
[UiO-67(bipy)Cu(H)in], **1g** [d]	-0.96	(f)	-1.04	-0.61	-0.65	-0.11	-0.15

Figure 4. DFT-calculated energy profile for the two reaction steps in the catalytic cycle for the model MOF system **1g**. Based on X-ray [21] quadratic structure of octahedron base, the struc… with resolution of identity method (W06) with def2-S… s labeled by green sticks, 1 (bipy*)Cu(H) chain and 4 Zr

[c] Potential energy diagra…
[d] Potential energy diagra…
[e] Potential energy diagra…
[f] Barrierless process as tr…

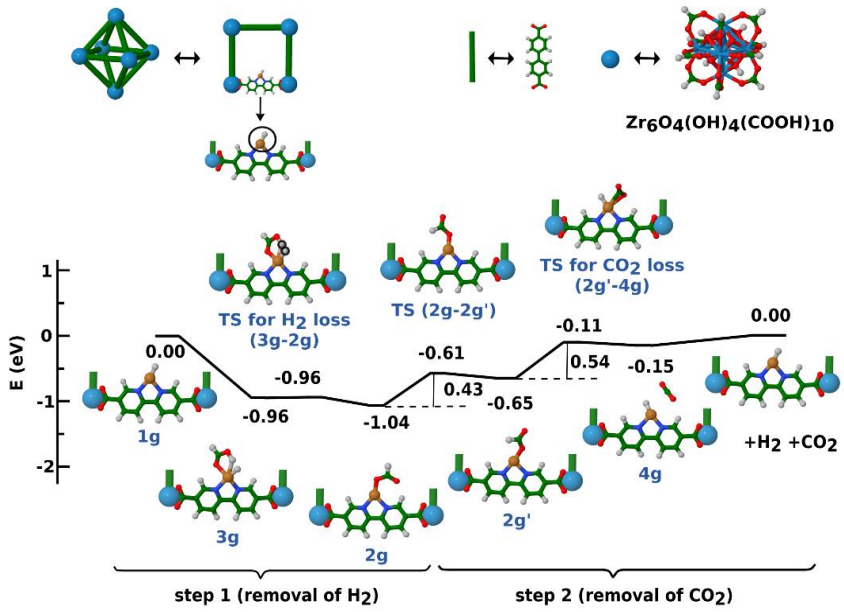

An examination of Table 1 reveals that some species related to the catalytic cycle are influenced by the electronic effects associated with the various ligands used in the different models. The phen*, bipy and bipy* ligands of the gas-phase models **1d**, **1e** and **1f** have little influence on the energetics for **3**, **TS3-2** and **2** associated with Step **I**, whereas species **TS2-2'**, **2'** and **TS2'-4** associated with step **II** are slightly higher for the gas-phase **1e** and **1f**. Comparing the gas-phase model **1f** to the MOF models **1g** and **1h** reveals that the MOF environment provides a cooperative effect in which the energetics of virtually all species becomes more favorable. This is likely due to electric field effects, which have generated much recent interest in enhancing organic reactions [22] but which appear to have been limited to discussions of the separation of gases in the context of MOFs [23]. It is worth noting that the Gibbs energies associated with key species for Steps I and II for 1d, 1f and 1g which are given in Table S1 show the same trends as the corresponding energies presented in Table 1.

Conclusion

Here we have extended the "heterogenization of a homogenous catalyst" strategy to use gas-phase studies to design a MOF based catalyst. In particular, we have used mass spectrometry experiments to model an organic linker with a {CuH} catalytic site and show that both steps of the catalytic cycle are selective for H_2 and CO_2 formation. DFT calculations have revealed that the mechanism associated with both steps of the catalytic cycle are essentially identical for three gas-phase models and are very similar to those of the two UiO-67 MOF models. Thus catalytic active sites located on the organic linker of MOFs appear to be close to a gas-phase environment, and thereby benefit from the favorable characteristics of gas-phase reactions. These include selectivity and enhanced rate of reaction due to lack of solvent effects [24]. Indeed if a MOF catalyst operates to process gaseous reactants and products, selectivity should be observed [25]. Our new conceptual approach opens routes towards the use of new MOF materials based on UiO-67 as novel catalysts for selective decomposition of formic acid into H_2 and CO_2. Studies are underway to prepare and evaluate the performance of such MOF catalysts [26].

Experimental Section

Mass spectrometry experiments: Gas-phase experiments on $[(phen^*)Cu(H)]^{2-}$, formed as discussed in the Supporting Information, were carried out using a Finnigan linear quadrupole (LTQ) mass spectrometer modified to allow the study of IMR [27,28]. The unimolecular fragmentation/dissociation of mass-selected $[(phen^*)Cu(O_2CH)]^{2-}$ occurred via CID using a normalized collision energy of 20 and an activation time of 30 ms. The CID isolation width was 1 *m/z*. IMRs were carried by delivering a measured concentration of formic acid into the helium bath gas.

Theoretical methods

Determination of energy profiles for reactions included searches for minima and transition states using the Gaussian suite of programs [29]. For the gas-phase models of $[(phen^*)Cu(H)]^{2-}$, 1d, [(bipy)Cu(H)], 1e and [(bipy*)Cu(H)] , 1f hybrid B3LYP [30] functional with def2-TZVP [31] atomic basis set were taken. The differences in the electronic energies are used rather than the ΔG for the following reasons due to the experimental conditions: (1) the ion-molecule reaction (step I) occurs under low-pressure conditions leading to unfavorable entropy effects arising from loss of degrees of freedom in the entrance channel where two gas-phase molecules react to form a single encounter complex [32]; (2) for the low energy CID reaction (step II) the effective temperature at which decarboxylation occurs is unknown since the precursor ions undergo multiple collisions with the helium bath gas resulting in slow "heating" until fragmentation occurs [33]. For the model MOF systems [UiO-67(bipy)Cu(H)in], 1g and [UiO-67(bipy)Cu(H)out], 1h, PBE [34] functional with resolution of identity method (W06) [35] in combination with def2-SVP [36] was used. Zirconium atoms have been treated with Stuttgart relativistic effective core potential [37] with corresponding atomic orbital basis set.

Acknowledgements

R.A.J.O. thanks Profs. Seth Cohen, Brendan Abrahams and Dr Carol Hua for valuable discussions and acknowledges funding from the Australian Research Council (project number DP180101187) and the Alexander Humboldt foundation for the award of a senior fellowship, which facilitated stimulating discussions on catalysis with a wide range of chemists. This research was partially supported by the project STIM – REI, Contract Number: KK.01.1.1.01.0003, funded by the European Union through the European Regional Development Fund – the Operational Programme Competitiveness and Cohesion 2014-2020 (KK.01.1.1.01). VBK, MK and AM acknowledge computational facility SRCE at the University of Zagreb as well as Prof. Miroslav Radman at MedILS and Split-Dalmatia County for support.

Keywords: MOF based catalyst • Formic Acid • Selective Decarboxylation • DFT calculations

[1] B. F. Hoskins, R. Robson, *J. Am. Chem. Soc.* **1989**, *111*, 5962−5964.
[2] B. F. Hoskins, R. Robson, *J. Am. Chem. Soc.* **1990**, *112*, 1546−1554.
[3] R. Robson, *Dalton Trans.* **2008**, 5113-5131.
[4] O. M. Yaghi, H. Li, *J. Am. Chem. Soc.* **1995**, *117*, 10401.
[5] S. M. Cohen, *J. Am. Chem. Soc.* **2017**, *139*, 2855−2863.
[6] C.-D. Wu, A. Hu, L. Zhang, W. Lin, *J. Am. Chem. Soc.* **2005**, *127*, 8940−8941.
[7] (a) Y.-B. Huang, J. Liang, X.-S. Wang, R. Cao, *Chem. Soc. Rev.* **2017**, *46*, 126; (b) J.-S. Qin, S. Yuan, C. Lollar, J. Pang, A. Alsalme, H.-C. Zhou, *Chem. Commun.* **2018**, *54*, 4231.
[8] (a) R. A. J. O'Hair, *Chem. Comm.* **2006**, 1469 – 1481; (b) R. A. J. O'Hair, N. J. Rijs, *Acc. Chem. Res.* **2015**, *48*, 329–340.
[9] A. Zavras, G. N. Khairallah, M. Krstić, M. Girod, S. Daly, R. Antoine, P. Maitre, R. J. Mulder, S.-A. Alexander, V. Bonačić-Koutecký, P. Dugourd, R. A. J. O'Hair, *Nat. Commun.* **2016**, *7*, 11746.
[10] A. Zavras, J. M. White, R. A. J. O'Hair, *Dalton Trans.* **2016**, *45*, 19408-19415.
[11] A. Zavras, M. Krstić, P. Dugourd, V. Bonačić-Koutecký, R. A. J. O'Hair, *ChemCatChem* **2017**, *9*, 1298–1302.
[12] M. Krstić, Q. Jin, G. N. Khairallah, R. A. J. O'Hair, V. Bonačić-Koutecký, *ChemCatChem* **2018**, *10*, 1173-1177.
[13] a) A. Noor, J. Li, G. N. Khairallah, Z. Li, H. Ghari, A. J. Canty, A. Ariafard, P. S. Donnelly, R. A. J. O'Hair, *Chem. Comm.* **2017**, *53*, 3854 - 3857; b) Y. Yang, A. Noor, A. J. Canty, A. Ariafard, P. S. Donnelly, R. A. J. O'Hair, *Organometallics*. **2019**, *38*, 424 – 435.
[14] In the absence of a catalyst, decomposition of formic acid proceeds via two competing primary pathways: decarboxylation to yield H_2 and CO_2 and dehydration to produce H_2O and CO. Although decarboxylation is slightly exothermic (by around 0.15 eV using experimental heats of formation from H. Y. Afeefy, J. F. Liebman, S. E. Stein "Neutral Thermochemical Data", in NIST Chemistry WebBook, NIST Standard Reference Database Number 69, Eds. P.J. Linstrom and W.G. Mallard, National Institute of Standards and Technology, Gaithersburg MD, 20899, https://doi.org/10.18434/T4D303, (retrieved March 27, 2019)), it suffers from a high activation barrier (Figure S1) and is thus the minor reaction channel. For lead experimental and theoretical references, see: a) K. Saito, T. Shiose, O. Takahashi, Y. Hidaka, F. Aiba, K. Tabayashi, *J. Phys. Chem. A* **2005**, *109*, 5352–5357; b) J.-G. Chang, H.-T. Chen, S. Xu, M. C. Lin, *J. Phys. Chem. A* **2007**, *111*, 6789–6797.
[15] M. Grasemann, G. Laurenczy, *Energy Environ. Sci.* **2012**, *5*, 8171–8181.
[16] For reviews covering aspects on the preparation and reactions of "ship-in-a-bottle" catalysts see: (a) G. A. Ozin, C. Gil, *Chem. Rev.* **1989**, *89*, 1749-1764; (b) M. Ichikawa, *Platinum Metals Rev.* **2000**, *44*, 3-14; (c) C. Li, *Catalysis Rev.* **2004**, *46*, 419-492.
[17] (a) L. Li, S. Tang, C. Wang, X. Lv, M. Jiang, H. Wua, X. Zhao, *Chem. Commun.* **2014**, *50*, 2304; (b) H. Fei, S. M. Cohen, *Chem. Commun.* **2014**, *50*, 4810.
[18] T. Toyao, K. Miyahara, M. Fujiwaki, T.-H. Kim, S. Dohshi, Y. Horiuchi, M. Matsuoka, *J. Phys. Chem. C* **2015**, *119*, 8131−8137.
[19] For reviews on the use of charged ligands in catalysis, see: a) D. M. Chisholm, J. S. McIndoe, *Dalton Trans.* **2008**, 3933-3945; b) J. Limberger, B. C. Leal, A. L. Monteiro, J. Dupont, *Chem. Sci.* **2015**, *6*, 77-94.
[20] Sulfonates are known to be amongst the weakest bases in the gas phase: J. D. Smith, R. A. J. O'Hair, T. D. Williams, *Phos. Sulf. Silicon Rel. Elements*, **1996**, *119*, 49-59. For example, the gas-phase basicity (anion proton affinity) of $PhSO_3^-$ is 13.4 eV while that of HCO_2^- is 15 eV (data from J. E. Bartmess, "Negative Ion Energetics Data" by in NIST Chemistry WebBook, NIST Standard Reference Database Number 69, Eds. P.J. Linstrom and W.G. Mallard, National Institute of Standards and Technology, Gaithersburg MD, 20899, https://doi.org/10.18434/T4D303, retrieved February 26, 2019).
[21] Crystal structure (CSD-1441659): a) C. R. Groom, I. J. Bruno, M. P. Lightfoot, S. C. Ward, *Acta Cryst.* **2016**, *B72*, 171-179; b) C. L. Hobday, R. J. Marshall, C. F. Murphie, J. Sotelo, T. Richards, D. R. Allan, T.

Düren, F.-X. Coudert, R. S. Forgan, C. A. Morrison, S. A. Moggach, T. D. Bennett, *Angew. Chem. Int. Ed.* **2016**, *55*, 2401.

[22] For lead references of electric field effects in organic chemistry, see: a) A. C. Aragonès, N. L. Haworth, N. Darwish, S. Ciampi, N. J. Bloomfield, G. G. Wallace, I. Diez-Perez, M. L. Coote, Nature, 2016, 531, 88–91; b) S. Shaik, R. Ramanan, D. Danovich and D. Mandal, *Chem. Soc. Rev.*, **2018**, *47*, 5125-5145; c) L. Yue, N. Wang, S. Zhou, X. Sun, M. Schlangen, H. Schwarz, Angew. Chem. Int. Ed., **2018**, *57*, 14635-14639.

[23] For a discussion of electric field effects in MOFs, see: C. H. Hendon, A. J. Rieth, M. D. Korzyński, M. Dincă, *ACS Cent. Sci.* **2017**, *3*, 554.

[24] C. H. DePuy, *J. Org. Chem.*, **2002**, *67*, 2393.

[25] A. B. Redondo, F. L. Morel, M. Ranocchiari, J. A. van Bokhoven, ACS Catal. 2015, 5, 7099−7103

[26] A reviewer has correctly pointed out that production of minor amounts (even at ppm levels) of CO from the decomposition of formic acid to CO and H_2O rather than CO_2 and H_2 will affect the performance of fuel cells. Although we find no evidence in the mass spectrum for CO formation in competition with decarboxylation of **2d** in step II of the catalytic cycle, the evaluation of the performance of MOF will require the analysis of all gaseous products to establish whether CO production is an issue.

[27] W. A. Donald, C. J. McKenzie, R. A. J. O'Hair, *Angew. Chem. Int. Ed.*, **2011**, *50*, 8379–8383

[28] a) S. Gronert, *J. Am. Soc. Mass Spectrom.*, **1998**, *9*, 845; b) W. A. Donald, G. N. Khairallah, R. A. J. O'Hair, *J. Am. Soc. Mass Spectrom.*, **2013**, *24*, 811-815.

[29] Gaussian 09 (Revision D.01): M. J. Frisch et al., Gaussian, Inc., *Wallingford CT*, **2013**.

[30] a) A. D. Becke, *Phys. Rev.* **1988**, *38*, 3098-3100; b) A. D. Becke, *J. Chem. Phys.* **1993**, *98*, 5648-5652; c) C. Lee, W. Yang, R. G. Parr, *Phys. Rev. B* **1988**, *37*, 785-789.

[31] A. Schäfer, C. Huber, R. Ahlrichs, *J. Chem. Phys.* **1994**, *100*, 5829-5835.

[32] S. A. McLuckey, D. E. Goeringer, *J. Mass Spectrom.* **1997**, *32*, 461-474.

[33] P. D. Dau, P. B. Armentrout, M. C. Michelini, J. K. Gibson, *Phys. Chem. Chem. Phys.* **2016**, *18*, 7334-7340.

[34] a) J. P. Perdew, K. Burke, M. Ernzerhof, *Phys. Rev. Lett.* **1996**, *77*, 3865-3868; b) J. P. Perdew, K. Burke, M. Ernzerhof, *Phys. Rev. Lett.* **1997**, *78*, 1396.

[35] a) F. Weigend, R. Ahlrichs, *Phys. Chem. Chem. Phys.* **2005**, *7*, 3297-3305; b) F. Weigend, *Phys. Chem. Chem. Phys.* **2006**, *8*, 1057-1065.

[36] a) A. Schäfer, H. Horn, R. Ahlrichs, *J. Chem. Phys.* **1992**, *97*, 2571; b) K. Eichkorn, F. Weigend, O. Treutler, R. Ahlrichs, *Theor. Chem. Acc.* **1997**, *97*, 119.

[37] D. Andrae, U. Haeussermann, M. Dolg, H. Stoll, H. Preuss, *Theor. Chim. Acta* **1990**, *77*, 123-141.

Entry for the Table of Contents

FULL PAPER

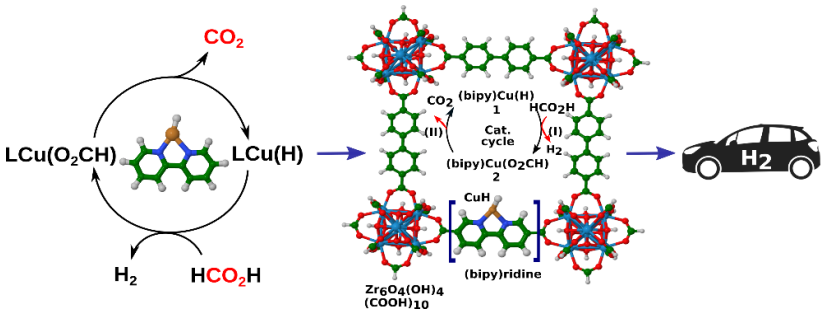

Richard A. J. O'Hair, Antonija Mravak, Marjan Krstić and Vlasta Bonačić-Koutecký**

Page No. – Page No.

Models facilitating the design of a new metal-organic framework catalyst for the selective decomposition of formic acid into hydrogen and carbon dioxide.